IEEE Access
Multidisciplinary | Rapid Review | Open Access Journal

Received April 8, 2019, accepted May 16, 2019, date of publication June 5, 2019, date of current version June 27, 2019.

Digital Object Identifier 10.1109/ACCESS.2019.2920945

Fast Multi-Objective Optimization of Multi-Parameter Antenna Structures Based on Improved BPNN Surrogate Model

JIAN DONG, (Member, IEEE), WENWEN QIN, AND MENG WANG, (Member, IEEE)
School of Computer Science and Engineering, Central South University, Changsha 410083, China

Corresponding author: Meng Wang (mwang2@csu.edu.cn)

This work was supported in part by the National Natural Science Foundation of China under Grant 61801521, in part by the Natural Science Foundation of Hunan Province under Grant 2018JJ2533, and in part by the Fundamental Research Funds for the Central Universities under Grant 2017gczd001.

ABSTRACT In this paper, a surrogate model based on a sparsely connected back propagation neural networks (SC-BPNN) is proposed to reduce the large computational cost of conventional multi-objective antenna optimization problems. In this model, the connection parameters and network structure can be adaptively tuned by a hybrid real-binary particle swarm optimization (HPSO) algorithm for better network global optimization capability. Also, a time-varying transfer function is introduced to improve the problem of easily trapping into local optimum and to accelerate network convergence. Further, a fast multi-objective optimization framework based on the proposed SC-BPNN is established for multi-parameter antenna structures. Finally, a Pareto-optimal planar miniaturized multiband antenna design is presented, indicating that the proposed model predicts antenna performance more accurately and saves considerable computational cost compared to those previously published approaches.

INDEX TERMS Antenna design, multi-objective optimization, surrogate model, BP neural network, HPSO, transfer function.

I. INTRODUCTION AND MOTIVATION

In recent years, different evolutionary algorithms (EAs), such as genetic algorithm (GA) [1], [2], particle swarm optimization (PSO) [3], [4], and nondominated sorting genetic algorithm (NSGA) [5], have been widely used in multi-parameter antenna or array configuration optimizations. Conventionally, commercial full-wave electromagnetic (EM) simulators are used to calculate the antenna response. However, optimization of an antenna configuration involves a huge amount of EM simulations, the process of which is computationally intensive and time–consuming. This poses a great challenge on fast antenna designs [6]. Therefore, enhancing the optimization speed while only sacrificing a small amount of simulation accuracy would be significant for fast antenna designs.

Fortunately, the recently developed surrogate-based optimization techniques [7]–[18] have proven to be more computationally efficient than traditional EM-driven methods. Compared with traditional EM-driven approaches, surrogate-based optimization techniques construct a mathematical model to predict the antenna performance, thereby greatly reducing the computational cost. Different surrogate models are proposed for antenna designs, such as Kriging [7]–[11], Gaussian Process (GP) [12], [13], and neural networks (NNs) [14]–[17]. The Kriging method used in [7]–[11] is essentially an interpolation method and the model prediction accuracy mostly depends on the initial sample, which may cause the model to either stop prematurely or search too locally [18]. The GP method used in [12] and [13] is still derived from the Kriging model [19] and retains some defects in the Kriging model. Recently, the Neural Network (NN) techniques have also been widely used in antenna designs [14]–[17] to obtain a surrogate model instead of a fine model which has high computational burden. Neural networks learn EM data through the training process and the trained neural networks are then used as fast and accurate surrogate models for complex antenna structure designs.

The associate editor coordinating the review of this manuscript and approving it for publication was Kai-Da Xu.

2169-3536 © 2019 IEEE. Translations and content mining are permitted for academic research only.
Personal use is also permitted, but republication/redistribution requires IEEE permission.
See http://www.ieee.org/publications_standards/publications/rights/index.html for more information.

In [14], a hybrid surrogate model consisting of the radial basis function neural networks (RBFNN) and the Kriging model was used to solve high-dimensional antenna optimization problems. However, in order to achieve a high prediction accuracy, the hybrid network structure is relatively complicated and requires increased training time, and tends to over-fit the training data instead of producing generalized results in the RBF network. In [15], a multi-layer perceptron neural network (MLP-NN) based model was constructed to simultaneously predict the size of the slot on the radiating patch and the size of the air-gap between the ground plane and the substrate sheet. In [16], an MLP-NN trained by backpropagation algorithm (MLP-BPNN) was used to relate the antenna's operating frequency with its dimensional parameters and then embedded into the loop of the single-objective particle swarm optimizer (PSO) to determine the optimal dimensions for a particular user-defined frequency. Also, an MLP-BPNN model was derived in [17] to design a dual-band, circularly-polarized slotted patch antenna, which allows obtaining antenna physical dimensions satisfying both near- and far-field goals (i.e., S_{11} and AR). The above work indeed reduced the design cycles of antenna optimization, but made few efforts on the particular NN design (i.e., network structure and connection parameters), which much affects the performance of antenna optimization.

Due to strong generalization ability and simple network structure, BPNN is suitable for modeling high-dimensional and highly nonlinear problems like antenna designs. However, the conventional BPNN faces some disadvantages: 1) the conventional BPNN has a fixed full-connected network structure with a large number of redundant connections. These redundant connections may cause the network structure to be unnecessarily complicated and not be beneficial to accurately mapping the input-output relationship, which results in excessive computation and is not favorable for convergence. 2) the number of the hidden layer nodes is derived from trial and error procedures or personal experience, which may not always show the best performance during a given training period [20]. A network with too few nodes may be unable to efficiently map input-output relationship. However, a network with too many nodes may become complex and require increased training time. 3) the performance of the conventional BPNN often depends on selection of initial network connection parameters (i.e., connection weights and thresholds). The commonly used random initialization network connection parameters will lead to network instability and make network training easy to fall into local optimization, which affects network prediction accuracy. To overcome the above drawbacks of conventional BPNN, we propose an innovative analysis methodology for fast prediction of the EM response of multi-parameter antenna structures.

As for the main innovative contributions of this paper, they include: 1) a new sparsely-connected BPNN (SC-BPNN) is proposed and hybrid real-binary particle swarm optimization (HPSO) [21] is used to tune the connection parameters and link states to improve the global optimization capability of the network; 2) a transfer function with a time-varying factor is introduced to reduce the possibility of model's trapping into local minima and to accelerate the network convergence; 3) by combining the proposed SC-BPNN model and multi-objective evolutionary algorithms (MOEAs), a fast multi-objective optimization framework for multi-parameter antenna structures is developed.

The rest of this paper is organized as follows. First, the problem of the multi-objective antenna design is mathematically formulated in Section II. Then, section III mainly describes the SC-BPNN based prediction method. In Section IV, we present a fast multi-objective antenna optimization framework based on SC-BPNN surrogate model, and Section V reports a design example of a miniaturized triple-band planar monopole antenna to demonstrate the effectiveness of the fast multi-objective design method based on SC-BPNN surrogate model. Finally, section VI concludes this paper.

II. PROBLEM FORMULATION

The multi-objective design of multi-parameter antenna structures can be generally stated as a multi-objective optimization problem (MOOP)

$$\begin{cases} \min\ F(\boldsymbol{x}) = (f_1(\boldsymbol{x}), f_2(\boldsymbol{x}), \ldots, f_{N_{obj}}(\boldsymbol{x}))^T \\ s.t.\ \ \boldsymbol{x} \in \boldsymbol{X} \end{cases} \tag{1}$$

where $\boldsymbol{x} = (x_1, \ldots, x_n) \in X \subset R^n$ is an n-dimensional design vector defining a particular antenna structure; $\boldsymbol{X}$ is a design space determined by the range of design parameters; and $f_k(\boldsymbol{x})$, $k = 1, 2, \ldots, N_{obj}$ is the kth design objective (e.g., reflection coefficient, gain, efficiency, antenna size, etc.), and $F(\boldsymbol{x}) \in \boldsymbol{R}^m$ is an N_{obj}-dimensional goal vector. Multi-objective antenna designs aims to find the Pareto front (PF) [9], i.e., multiple designs indicating the trade-off among various antenna specifications under consideration.

For an MOOP, any two designs $\boldsymbol{x}^{(1)}$ and $\boldsymbol{x}^{(2)}$ for which $f_k(\boldsymbol{x}^{(1)}) < f_k(\boldsymbol{x}^{(2)})$ and $f_l(\boldsymbol{x}^{(1)}) < f_l(\boldsymbol{x}^{(2)})$ for at least one pair $k \neq l$, are not commensurable, that is, none is better than the other in the multi-objective sense [9]. Thus, we define the Pareto dominance relation $\prec$ as: for the two designs $\boldsymbol{x}^{(1)}$ and $\boldsymbol{x}^{(2)}$, we have $\boldsymbol{x}^{(1)} \prec \boldsymbol{x}^{(2)}$($\boldsymbol{x}^{(1)}$ dominates $\boldsymbol{x}^{(2)}$) if $f_k(\boldsymbol{x}^{(1)}) \leq f_k(\boldsymbol{x}^{(2)})$ for all $k = 1, 2, \ldots, N_{obj}$ and $f_k(\boldsymbol{x}^{(1)}) < f_k(\boldsymbol{x}^{(2)})$ for at least one k [9]. In an MOOP, we want to find a representation of a so-called PF $\boldsymbol{X}_p$ (viz. Pareto-optimal set) of the design space $\boldsymbol{X}$, such that for any $\boldsymbol{x} \in \boldsymbol{X}_p$, there is no $\boldsymbol{x}' \in \boldsymbol{X}$ for which $\boldsymbol{x}' \prec \boldsymbol{x}$ [9], [22].

III. ANTENNA SURROGATE MODEL BASED ON SC-BPNN

In this section, we first briefly describe the conventional BPNN for antenna design. Then, to avoid the drawbacks of the conventional BPNN, a novel sparsely-connected BPNN (SC-BPNN) model is proposed, including the tuning of connection parameters and network structure and the design of the transfer function with a time-varying transfer factor.

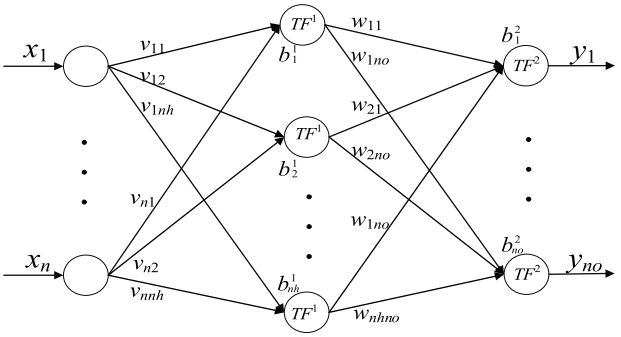

FIGURE 1. The structure of a conventional three-layer BPNN.

A. CONVENTIONAL BPNN MODEL

BPNN, proposed by Rumelhart et al. [23], is a multi-layer feedforward neural network model with strong generalization capability. A three-layer feedforward NN can approximate any nonlinear continuous function to an arbitrary accuracy [24]. The structure of a three-layer BPNN is shown in Fig. 1, where the input-output relationship can be formulated as

$$y_k = TF^2\left(\sum_{j=1}^{nh}(w_{jk}TF^1(\sum_{i=1}^{n}v_{ij}x_i - b_j^1) - b_k^2)\right),$$
$$k = 1, 2, \ldots, no \tag{2}$$

where x_i is the input of the BPNN and represents the ith design variable of a particular antenna structure; y_k is the output of the BPNN and represents the kth component of a particular performance index (e.g., the S_{11} value at the kth frequency point); n is the number of inputs and also the number of design variables; nh is the number of the hidden layer nodes; no is the number of outputs; v_{ij} denotes the link weight between the ith input and the jth hidden node; w_{jk} denotes the link weight between the jth hidden node and the kth output; b_j^1 and b_k^2 denote the biases for the hidden and output nodes, respectively; TF^1 and TF^2 are the transfer functions of the hidden layer and the output layer, respectively. Generally, TF^1 is the sigmoid function and TF^2 is the linear function.

For the traditional EAs-based antenna optimization methods, it is time-consuming to find an optimal antenna solution satisfying specific performance requirements as they usually need hundreds or even thousands of EM simulations. By using BPNN as a surrogate model during the optimization process, it can greatly reduce the time on computing antenna response and hence improve the efficiency of antenna optimization. The role of a BPNN surrogate model is to form a mapping between the design parameters of a particular antenna structure and its antenna performance indexes (e.g., reflection coefficients, gain, efficiency, etc.), which is equivalent to form a black box between the antenna design parameters and performance indexes as shown in Fig. 2.

B. SPARSELY-CONNECTED BPNN MODEL

When constructing the BPNN antenna surrogate model, the BP algorithm based on gradient descent often relies on the

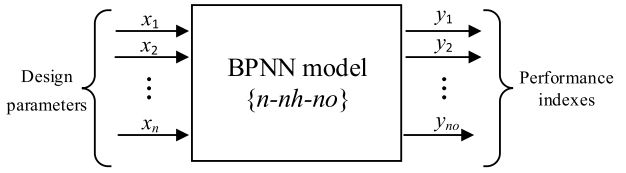

FIGURE 2. Black box for evaluation of antenna performance.

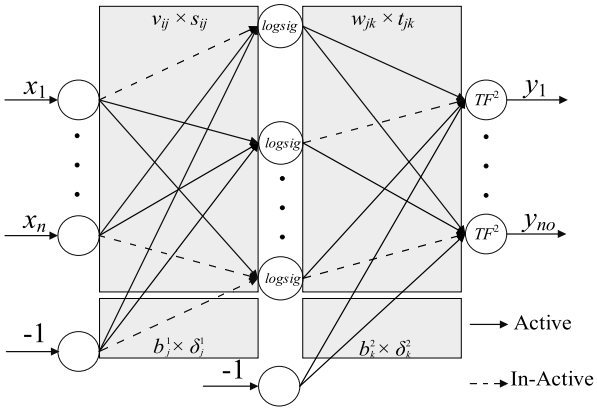

FIGURE 3. The structure of the proposed SC-BPNN.

selection of network parameters such as initial weights (w_{jk} and v_{ij}) and thresholds (b_j^1 and b_k^2) [23], [25]. The commonly used random initialization of network connection parameters will lead to network instability and make network training easy to fall into local optimum. Moreover, the conventional BPNN usually has a fixed full-connected network structure that does not properly map the input-output relationship for the particular application. The redundant connection may result in excessive computation and not be favorable for convergence. In addition, the empirically derived hidden layer nodes may not always provide the best network convergence performance during a given training period [20].

Therefore, a new sparsely-connected BPNN (SC-BPNN) model is given in Fig. 3. As shown in Fig. 3, s_{ij}, t_{jk}, δ_j^1, δ_k^2 are introduced to determine the states of links between nodes, with a value of 0 or 1. If the structure parameter value is 1, it means that the link is active and is indicated by a solid line. Otherwise, the dotted line in Fig. 3 indicates that the structure parameter is 0 and the link is in-active. In addition, nodes with an input value of -1 are added to the input layer and the hidden layer to adjust thresholds of the hidden layer and output layer, respectively. Different from the conventional BPNN model, both connection parameters and link states can be optimized to simplify the input-output mapping relationship of SC-BPNN, thus facilitating the improvement of network prediction accuracy.

The input-output relationship of the SC-BPNN can be formulated as

$$y_k = TF^2\left(\sum_{j=1}^{nh}(w_{jk}t_{jk}\log\mathrm{sig}(\sum_{i=1}^{n}v_{ij}s_{ij}x_i - b_j^1\delta_j^1) - b_k^2\delta_k^2)\right),$$
$$k = 1, 2, \ldots, no \tag{3}$$

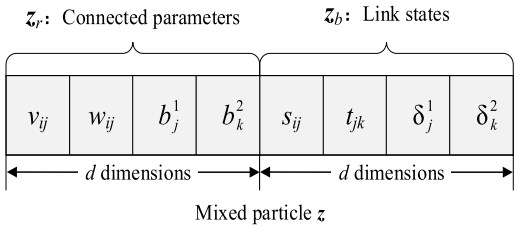

FIGURE 4. The structure of a mixed particle *z*.

where logsig $(\cdot)$ is the transfer function f^1 and defined as

$$\log\text{sig}\,(x_i) = \frac{1}{1+e^{-x_i}}, \quad x_i \in \Re. \tag{4}$$

Next, we tune the connection parameters and link states by using an HPSO to compact network structure and optimize network performance. Also, we modify the transfer function TF^1 by introducing a time-varying factor to improve the global optimization ability and speed up the convergence.

1) TUNING OF CONNECTION PARAMETERS AND NETWORK STRUCTURE by HPSO

The connection parameters and network structure optimization problem in the SC-BPNN model can be described as:

$$\begin{aligned} find\, \boldsymbol{z}_{op} &= \arg\max_{z=(z_r,z_b)} g(\boldsymbol{z}), \\ & s.t.\, \boldsymbol{z}_r \in (0,1)^d, \quad \boldsymbol{z}_b \in [0,1]^d \end{aligned} \tag{5}$$

where $\boldsymbol{z} = (\boldsymbol{z}_r, \boldsymbol{z}_b)$ is a mixed particle as shown in Fig. 4; the real number part $\boldsymbol{z}_r \in (0,1)^d$ is a vector of floating numbers including all the connection parameters; the binary number part $\boldsymbol{z}_b \in [0,1]^d$ represents all the link states, and each dimension of $\boldsymbol{z}_b$ has a value of 0 or 1 (0 means the link state is in-active and 1 means the link state is active); the total dimension d of $\boldsymbol{z}_r$ and $\boldsymbol{z}_b$ is determined by

$$d = n \times nh + nh \times no + nh + no \tag{6}$$

Note that, the total dimension of the mixed particle is expanded dynamically with the increasing number of hidden layer nodes nh. $\boldsymbol{z}_{op}$ is the optimal solution to be determined and ultimately used to construct the antenna surrogate model; $g(\boldsymbol{z})$ is the scalar fitness function defined by

$$g = \frac{1}{1+\boldsymbol{err}} \tag{7}$$

where ***err*** is the mean absolute error (MAE) defined as

$$\boldsymbol{err} = \sum_{t=1}^{q} \frac{\sum_{k=1}^{no} |Y_k(t) - y_k(t)|}{no \times q} \tag{8}$$

where q is the number of input samples; $Y_k\,(t)$ is the response output of each group of input samples, and $y_k\,(t)$ is the predicted response output of SC-BPNN for each set of input samples. It can be seen from (7) and (8) that a larger fitness value implies a smaller error value.

In order to determine the appropriate network, an HPSO [21] is adopted for optimizing the connection parameters and link states. The main procedures are summarized as follows:

Step 1. Determine network training parametersč"

Step 1.1. Determine the range of the number of hidden layer nodes, i.e., $nh_{\min}$ and $nh_{\max}$;

Step 1.2. Set the termination condition, i.e., the predetermined accuracy ε and the maximum number of iterations;

Step 2. Set $nh = nh_{\min}$, encode and initialize the mixed particle swarm $\boldsymbol{z} = (\boldsymbol{z}_r, \boldsymbol{z}_b)$;

Step 3. Calculate the initial scalar fitness $g(\boldsymbol{z})$;

Step 4. Update the mixed particle swarm according to the update method of HPSO;

Step 5. Evaluate the mixed particle and update ***gbest***, ***pbest***.

Step 6. Turn to step 5 when the termination condition is not satisfied, otherwise continue;

Step 7. Update the number of hidden layer nodes (i.e., $nh \leftarrow nh + 1$) to generate a new mixed particle swarm and go to step3.

Step 8. Compare the ***gbest*** corresponding to each value of nh, select the maximum ***gbest*** and output the optimal solution $\boldsymbol{z}_{op}$.

2) MODIFIED TRANSFER FUNCTION with a TIME-VARYING FACTOR

After the network structure and connection parameters of BPNN are determined, the network error is mainly determined by the transfer function. Different transfer functions present diverse behaviors and have different effects on the performance of the network [26]. The logsig $(\cdot)$ given by (4) is used in our proposed SC-BPNN model, which is responsible for limiting the output amplitude of the neurons and restricting the input data to a limited range of values. We summarize some useful principles that should be taken into account when designing the transfer function of BPNN as follows:

i) The transfer function should be continuous, monotonous, and differentiable, as the adjustment of the weight is proportional to the gradient of the error in the reverse learning algorithm of BPNN.

ii) The input of the transfer function is the dot product of the weight vector and the input vector, so its domain should be $(-\infty, +\infty)$.

iii) The role of the transfer function is to limit the output amplitude of the neurons, so the return values of a transfer function should be restricted within the segment [0, 1].

Fig. 5 presents some transfer function curves with different coefficients in order to investigate their effects on improving BPNN performance. It is observed that all transfer curves are monotonically increasing functions. Also, the larger the coefficient is, the steeper the transfer curve becomes. As the input value x rises, the curve with a larger coefficient approaches to its saturation much faster than that with a smaller coefficient does; that is, a transfer function with a larger coefficient experiences a steeper change in output value $s(x)$, and vice versa. Therefore, in the early stage of the training, setting a relatively smaller coefficient means that the transfer function

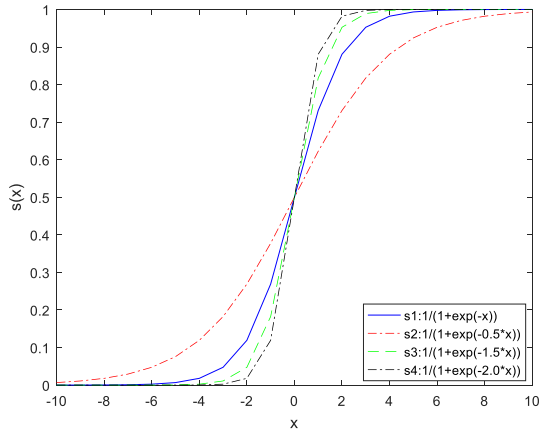

FIGURE 5. Transfer function curves with different coefficients.

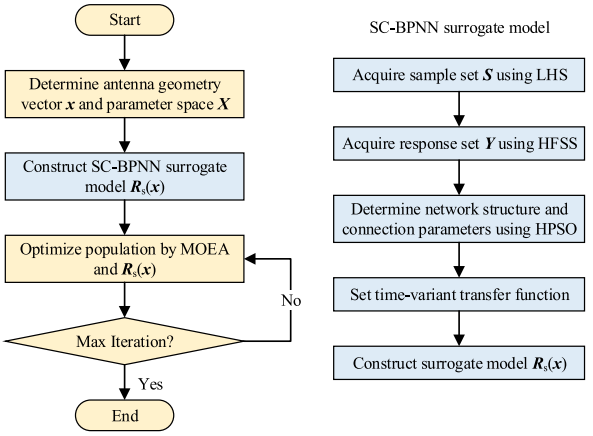

FIGURE 6. Flowchart of the fast multi-objective antenna optimization framework combining the SC-BPNN surrogate model and MOEAs.

curve is more flat and helps to improve the search accuracy of the network. As the training process goes on, the coefficient is grown to be larger for a steeper TF curve. This facilitates the model jumping out of the local minimum and speeding up convergence. So, a transfer function with a time-varying transfer factor is chosen. The modified transfer function can be expressed as

$$TF\left(x_i\left(k\right)\right) = \frac{1}{1+e^{-\alpha(k)x_i(k)}} \tag{9}$$

$$\alpha\left(k\right) = \alpha_{\max} - \frac{\alpha_{\max}-\alpha_{\min}}{k} \tag{10}$$

where $\alpha\left(k\right)$ is the transfer factor at the kth iteration, $\alpha_{\max}$ and $\alpha_{\min}$ are the maximum and minimum transfer factors, respectively.

IV. FAST MULTI-OBJECTIVE ANTENNA OPTIMIZATION FRAMEWORK BASED ON SC-BPNN SURROGATE MODEL

The traditional antenna design methods based on full-wave EM simulations are usually time-consuming due to repeated parameter sweeping processes, which limits their applications in complex multi-parameter antenna structure design problems. In this section, a fast multi-objective optimization framework combining multi-objective evolutionary algorithms (MOEAs) and the proposed SC-BPNN antenna surrogate model is developed for multi-parameter antenna structure designs. In this framework, each individual consists of n structural parameters to be optimized in the antenna design, which define a specific antenna structure. The SC-BPNN antenna surrogate model is used to replace the computationally expensive full-wave EM simulation for evaluating the individual fitness value. The fitness function is related to antenna performance indexes, such as reflection coefficients, gain, etc.

When constructing the SC-BPNN antenna surrogate model, Latin Hypercube Sampling (LHS) [27], [28] is first adopted to obtain the sample set $\boldsymbol{S} = [s_1, s_2, \cdots, s_q]^T, s_i \in \boldsymbol{R}^n$ in the antenna design space, and the EM simulator is used to obtain the high fidelity response set $\boldsymbol{Y}$ of these samples. Compared to randomized sampling, LHS can make the sample points fill the entire parameter space relatively evenly by layering and non-overlapping random sampling of parameter intervals. Next, an HPSO algorithm is used to tune the connection parameters and link states of SC-BPNN for obtaining the optimal solution z_{op}. Then, a time-varying transfer function is set to reduce the possibilities of the model falling into local minima and to accelerate convergence in BPNN. Finally, the sample set $\boldsymbol{S}$ and response set $\boldsymbol{Y}$ are utilized to construct an antenna surrogate model $\boldsymbol{R}_s(\boldsymbol{x})$.

Therefore, the fast multi-objective antenna design framework combining the SC-BPNN surrogate model and MOEAs can be summarized as follows:

1. Predefine the antenna geometry vector $\boldsymbol{x}$ and parameter space $\boldsymbol{X}$;
2. Obtain the sample set $\boldsymbol{S}$ by adopting LHS to sample parameter space and calculate the response set $\boldsymbol{Y}$ through EM simulations;
3. Determine network structure and connection parameters using HPSO;
4. Set a transfer function with a time-varying transfer factor;
5. Construct an SC-BPNN antenna surrogate model $\boldsymbol{R}_s(\boldsymbol{x})$;
6. Optimize the population using MOEAs and $\boldsymbol{R}_s(\boldsymbol{x})$;
7. Stop when the termination condition is satisfied; otherwise, turn to step 6.

The flowchart of the fast multi-objective antenna optimization framework combining the SC-BPNN surrogate model and MOEAs is shown in Fig. 6.

V. EXPERIMENTS AND DISCUSSIONS

In this section, the predicted results of the reflection coefficients of a planar monopole antenna obtained by our proposed SC-BPNN model are given and compared with those obtained by other surrogate models. Then, a miniaturized planar triple-band antenna design is presented to illustrate the fast multi-objective antenna optimization framework.

A. SC-BPNN ANTENN SURROGATE MODEL

The initial structure of the planar monopole antenna is shown in Fig. 7. This antenna is formed by a fork-shaped radiator

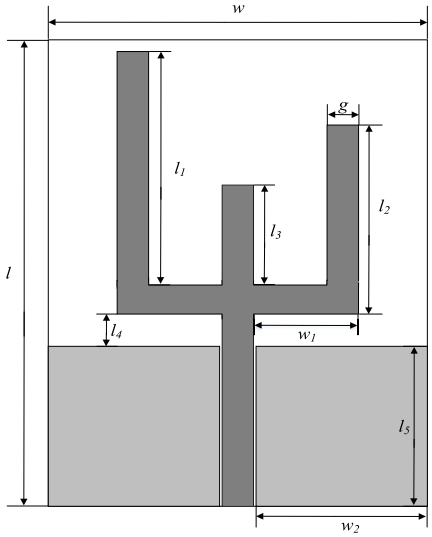

FIGURE 7. Geometry of the planar multiband antenna.

TABLE 1. Initial ranges of design parameters (units: mm).

Parameter	l	l_1	l_2	l_3	l_4
Range	[36,40]	[16,19]	[10,12.5]	[8.5,10.5]	[2.8,3.9]
Parameter	l_5	w	w_1	w_2	g
Range	[9.5,11.5]	[19,24]	[6.5,8.3]	[8.7,11.2]	[1.8,2.1]

and a rectangle ground plane, which can produce different resonant frequency bands to satisfy multi-band applications. The antenna is printed on a Rogers RO4003(tm) substrate of thickness 0.5mm, permittivity 3.55, and loss tangent 0.0027. Design variables are $\boldsymbol{x} = [l\ \ l_1\, l_2\, l_3\ \ l_4\, l_5\, w\, w_1\, w_2\, g\,]^T$. The initial ranges of design variables are listed in Table 1.

The LHS algorithm is used to generate a uniformly distributed sample set $\boldsymbol{S}$ within a given design space. It should be mentioned that the construction of highly accurate surrogate models usually needs a large number of samples, implying very high computational cost because of the involvement of extensive EM simulations. In our surrogate model, the predicted values of the reflection coefficients are only to properly reflect the trends of the S_{11} curve instead of providing exactly accurate predictions on the reflection coefficients. Therefore, after considering the trade-off between construction cost and prediction accuracy, the number of sample points is chosen to be 200, and the first 190 sample points are used for training, and the last 10 sample points are used for testing. All sample points are transmitted by the HFSS-MATLAB-API to HFSS through a function call to obtain the reflection coefficient response set $\boldsymbol{Y}$. Meanwhile, the early stopping method integrated in the MATLAB Neural Network Toolbox is used to mitigate the effects of overfitting. The number of input nodes n of the BPNN model is consistent with the number of antenna design variables to be optimized ($n = 10$ in this example), and the number of output nodes no is the same as the number of frequency points at which S_{11} values are predicted ($no = 15$ in this example), and the number of hidden nodes nh varies from 10 to 20. By using the sample set

TABLE 2. Comparison of fitness values for predicting the S_{11} values.

nh	SC-BPNN		Conventional BPNN		PSO-BPNN	
	Fitness Values	Number of Links	Fitness Values	Number of Links	Fitness Values	Number of Links
10	0.9465	96	0.8892	275	0.9190	275
11	0.9495	148	0.8781	301	0.8879	301
12	0.9476	175	0.8971	327	0.9074	327
13	0.9482	177	0.9056	353	0.9313	353
14	0.9507	183	0.9022	379	0.9147	379
15	0.9464	226	**0.9130**	**405**	0.9203	405
16	0.9430	209	0.8975	431	0.9138	431
17	**0.9508**	**238**	0.9087	457	0.9312	457
18	0.9408	278	0.8909	483	**0.9383**	**483**
19	0.9452	228	0.8925	509	0.9205	509
20	0.9446	289	0.9053	535	0.9226	535

TABLE 3. Comparison of errors and training times corresponding to different transfer factor ranges.

$\alpha_{\max}, \alpha_{\min}$	Minimum error	Mean error	Mean number of trainings
1.0,1.0	0.001523	0.002174	128.20
1.1,0.9	0.001484	0.002103	119.73
1.2,0.8	0.001441	0.001934	88.43
1.3,0.7	0.001452	0.001972	104.63
1.4,0.6	0.001084	0.001754	137.97
1.5,0.5	0.001200	0.001775	146.00

$\boldsymbol{S}$ and the response set $\boldsymbol{Y}$, we construct the SC-BPNN antenna surrogate model.

According to the parameter setting experience in [20] and [21], the HPSO parameters are set as follows: the number of particles is set as 50; the maximum generation is set as 2000; the learning factors $c_1 = c_2 = 1.49$; the real number part of inertia weight ω decreases linearly from 0.9 to 0.3 and the binary number part of ω is a constant 1.0; the maximum values of the real part and binary part of velocities are set to 0.1 and 6.0, respectively. In order to compare the performance of the proposed SC-BPNN with the conventional BPNN [16], [17], and the BPNN only adjusting its connection parameters by PSO (PSO-BPNN) [29], the experiments are performed for 30 times, and the results including best fitness values and the number of links are listed in Table 2. It is observed from Table 2 that the SC-BPNN provides better results in terms of fitness values and the number of links. The optimal result of SC-BPNN is obtained when the number of hidden layer nodes is 17 and the number of links is 238. Compared to the conventional BPNN and PSO-BPNN, the number of links is almost half reduced.

Next, the time-variant transfer function of the proposed BPNN is designed with $nh = 17$ and the number of links 238. By setting different values of α_{max} and α_{min}, the experiments are performed for 30 times, and the results including the minimum error values, the mean error values, and the average number of trainings are tabulated in Table 3 (the error refers to the MSE). It is observed from Table 3 that both the minimum errors and the mean errors of all transfer functions with the time-variant transfer factor (i.e., lower five rows) are smaller than those of the original fixed transfer

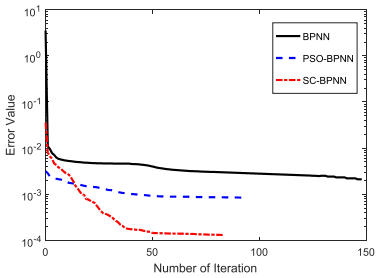

FIGURE 8. Training error curves of BPNN, PSO-BPNN and SC-BPNN.

function ($\alpha_{max} = \alpha_{min} = 1$). Also, the larger the varying range of transfer factor, the smaller the minimum error and the mean error. As the varying range of transfer factor increases, the mean number of trainings decreases firstly and then increases. The above results fully verify the design principle in Section III-B, that is, a relatively smaller transfer factor helps to improve the search accuracy of the network but leads to an increase in the number of trainings, and a larger transfer factor helps to jump out of the local minimum and speed up convergence. Considering both mean errors and number of trainings, the transfer factors with $\alpha_{max} = 1.2$ and $\alpha_{min} = 0.8$ are chosen. Thus, the proposed time-variant transfer function can reduce training errors and accelerate convergence.

After determining the network structure, connection parameters, and the transfer factors, the antenna surrogate model based on SC-BPNN is constructed. Fig. 8 shows the training error curves of conventional BPNN, PSO-BPNN, and our proposed SC-BPNN. It can be seen from Fig. 8 that the training error and the number of the required iterations are much smaller than those of the conventional BPNN [16], [17], and PSO-BPNN [29], indicating that our model can achieve a much lower training error at a faster convergence speed. This owes to the optimized connection parameters and simplified network structure and also the time-varying transfer function in the proposed SC-BPNN.

To further assess and summarize the differences among these models, Fig. 9 reports the scatter plots of the predicted results by Kriging [7], conventional BPNN [16], [17], PSO-BPNN [29], and our proposed SC-BPNN relative to the actual results obtained by HFSS. As it can be observed, the points in Fig. 9(a) are more concentrated on the diagonal compared to Fig. 9(b), Fig. 9(c), and Fig. 9(d), indicating SC-BPNN is significantly better than Kriging, conventional BPNN and PSO-BPNN in terms of prediction accuracy with the same number of sample points and hidden layer nodes. Note that, the Kriging model, as a comparison group, is trained before use as the BPNN models do. If we want to obtain a high-precision global model by Kriging, more initial sample points need to be added or the sample points should be dynamically updated during the optimization process [10]. Similarly, the conventional BPNN and PSO-BPNN need more implementation cost to achieve the same prediction accuracy as SC-BPNN, such as increasing initial sample points or further optimizing parameters. Also, Table 4 gives a comparison of the computational time of various surrogate

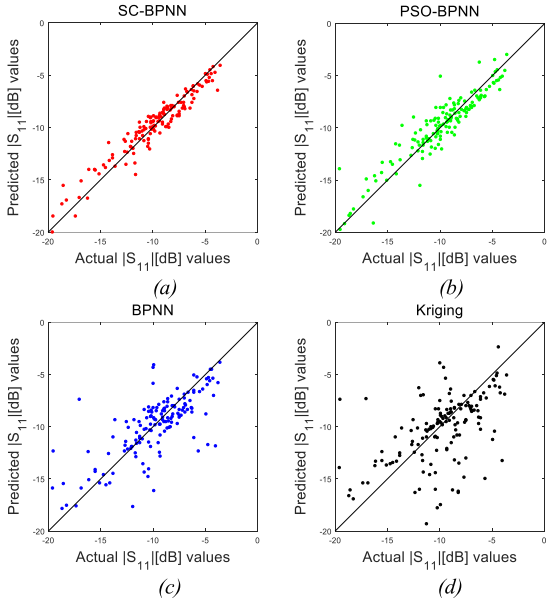

FIGURE 9. Comparison of actual versus predicted $|S_{11}|$ values when using (a) SC-BPNN, (b) PSO-BPNN, (c) BPNN, (d) Kriging surrogate models.

TABLE 4. Computational time of various surrogate models and HFSS simulations.

Model	HFSS	Kriging	BPNN	PSO-BPNN	SC-BPNN
Total time (s)	587.82	1.92	0.36	0.28	0.23
Average time(s)	58.78	0.192	0.036	0.028	0.023

models and HFSS simulations. The results in Table 4 show that the use of surrogate models greatly reduces the computational time compared to HFSS simulation.

In brief, for a given antenna structure, the proposed SC-BPNN can efficiently replace EM simulation software for antenna performance prediction and achieve a rapid antenna optimization with the aid of EAs.

B. PARETO-OPTIMAL DESIGNS of MINIATURIZED MULTIBAND ANTENNA

The multi-objective optimization of the given planar multiband antenna structure in Fig. 7 is implemented by using MOEA/D [30] and the SC-BPNN surrogate model constructed in Section V-A. Two design goals are to be achieved: (i) the reflection coefficient values ($|S_{11}|$) are below -10dB within the frequency bands of 2.40∼2.60GHz, 3.30∼3.80GHz, 5.00∼5.85GHz, covering the entire WLAN2.4/5.2/5.8GHz and WiMAX3.5GHz bands (objective F_1); (ii) the antenna structure is miniaturized to fit into portable devices (objective F_2). The objective function of F_1 is specified as

$$F_1 = \frac{1}{N}\sum_{i=1}^{n} Q(f_i) \tag{11}$$

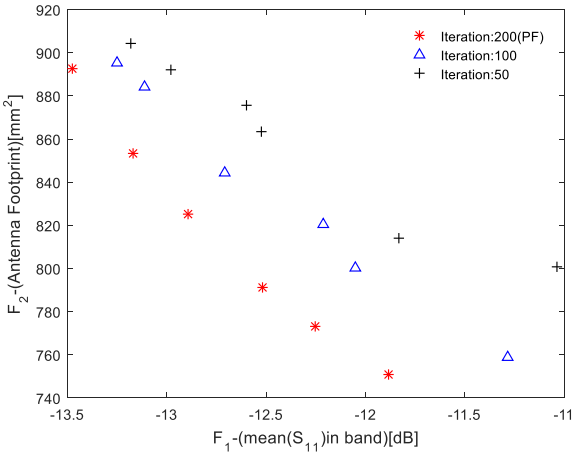

FIGURE 10. The obtained representations of the Pareto set during the optimization process for the planar miniaturized multiband antenna.

$$Q(f_i) = \begin{cases} |S_{11}(f_i)| & |S_{11}(f_i)| > -10 \\ -10 & |S_{11}(f_i)| \leq -10 \end{cases} \tag{12}$$

where f_i is the ith sample within the given operation bands; $S_{11}(f_i)$ is the reflection coefficient at f_i; N is the total number of sampling frequencies. The objective function of F_2 is defined as

$$F_2 = w \times l \tag{13}$$

Based on the parameter selection principle of MOEA/D in [30] and experiment experiences, the size of the randomly initialized population is set as 100, and the maximum iteration number is set as 200. The representations of the Pareto set for the miniaturized tri-band antenna during the optimization process are shown in Fig. 10, which displays the evolution behavior of the objective functions. The Pareto-optimal designs' corresponding $|S_{11}|$ values obtained by HFSS simulation and SC-BPNN surrogate model are shown in Fig. 11 and the detailed antenna designs are given in Table 5. Fig. 11 show that the predicted points by SC-BPNN surrogate model well match the trend of the HFSS simulation curve. Also, it is observed that the S_{11} curve is lower than -10dB within the three frequency bands of 2.33-2.66GHz, 3.05-3.89GHz, and 4.94-6.05GHz, satisfying the WLAN and WiMAX applications simultaneously. Thus, all of these designs are able to provide versatile choices for practical antenna applications.

To validate the effectiveness of SC-BPNN, Table 6 shows the results of F_1 for those chosen Pareto-optimal designs obtained by different surrogate models. The predictive results I and predictive results II are obtained by the conventional BPNN and SC-BPNN, respectively. Also, the error rates of the two prediction results with respect to HFSS simulations are given, separately. Table 6 shows that the prediction results of our proposed SC-BPNN (average error rate 2.25%) are significantly better than those of the conventional BPNN (average error rate 7.00%).

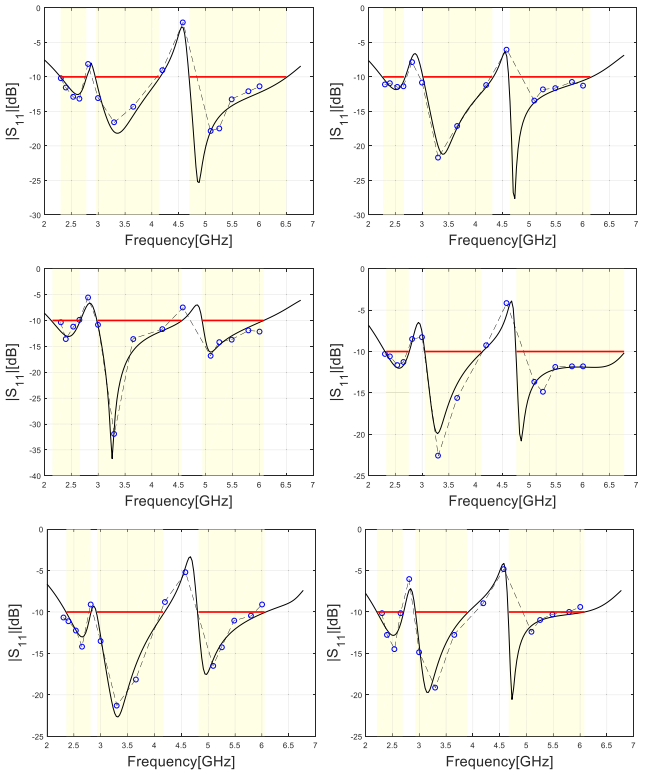

FIGURE 11. Simulated (—) and predicted (o) reflection responses for the obtained representations of the Pareto set for the planar miniaturized multiband antenna (from top left to bottom right): $x^{(1)}$, $x^{(2)}$, $x^{(3)}$, $x^{(4)}$, $x^{(5)}$, and $x^{(6)}$.

TABLE 5. Planar multiband antenna: Selected pareto-optimal designs.

Design	$x^{(1)}$	$x^{(2)}$	$x^{(3)}$	$x^{(4)}$	$x^{(5)}$	$x^{(6)}$
$F_1[dB]$	-13.47	-13.17	-12.89	-12.51	-12.25	-11.89
$F_2[mm^2]$	892.40	853.20	829.44	792.48	778.09	746.63
l	38.8	39.5	38.4	38.1	39.1	37.9
l_1	19.0	17.6	16.8	17.2	16.8	16.8
l_2	12.3	11.7	12.1	11.8	11.5	12.1
l_3	10.1	10.1	9.8	10.1	9.0	9.8
l_4	3.0	3.5	3.3	3.0	3.0	3.3
l_5	9.6	9.8	9.6	10.3	10.6	9.6
w	23.0	21.6	21.6	20.8	19.9	19.7
w_1	6.8	6.6	7.7	7.4	6.9	7.6
w_2	10.7	9.9	10.0	9.6	9.2	8.7
g	1.9	2.0	2.0	1.9	2.0	1.9

Further, we compare the proposed SC-BPNN with other techniques in terms of computation time. One EM simulation takes about 59 seconds under running environment equipped with a 64-bit operating system, 4GB RAM and 3.20GHz i5 processor. This work uses only 1.13% of the time cost of direct MOEA/D-based optimization without surrogate model (scheme I), and MOEA/D-based optimization with the conventional BPNN (scheme II) are about 1.03% of the time cost of scheme I. Compared MOEA-D with the conventional BPNN, the SC-BPNN surrogate model only takes slightly more time due to the extra time spent on HPSO tuning in

TABLE 6. Comparison of fitness values F_1 of selected pareto-optimal designs obtained by surrogate models and HFSS.

Design	$x^{(1)}$	$x^{(2)}$	$x^{(3)}$	$x^{(4)}$	$x^{(5)}$	$x^{(6)}$
Simulation results	-13.65	-12.74	-13.11	-12.78	-11.93	-12.17
Predictive results I	-14.31	-13.79	-14.08	-11.34	-12.65	-12.68
Predictive results II	-13.47	-13.17	-12.89	-12.51	-12.25	-11.89
Error rate I(%)	4.84	8.24	7.40	11.27	6.04	4.19
Error rate II(%)	1.32	3.38	1.68	2.11	2.68	2.30

TABLE 7. Comparison of computational cost among different antenna optimization schemes.

Optimization approach	Number of EM simulations	CPU Time /h	
		Total	Relative (%)
Scheme I	20000	327.88	100
Scheme II	200	3.38	1.03
This work	200	3.71	1.13

this work. The detailed time cost is given in Table 7. It can be seen that the overall CPU-time required by our technique and scheme II is considerably lower than scheme I. Although the computational cost of our method is slightly larger than that of scheme II, the prediction accuracy is much higher than that of scheme II as is observed from Table 6. In brief, the proposed technique can provide versatile desired antenna designs with affordable computational cost, thereby improving the antenna design cycle.

VI. CONCLUSION

An efficient technique based on an improved BPNN surrogate model is proposed to implement the fast multi-objective multi-parameter antenna optimization in this paper. To overcome the drawbacks of the conventional BPNN, a new sparsely-connected BPNN (SC-BPNN) model is proposed. Rather than a fixed network structure, this SC-BPNN model dynamically tunes the link states and connection coefficients between the nodes. By integrating the SC-BPNN surrogate model with MOEAs, a fast multi-objective antenna optimization framework is established. The Pareto-optimal designs of a compact tri-band planar monopole antenna are given, indicating that the proposed technique gives higher prediction accuracy and significant reductions of antenna optimization cost compared to other existing antenna structure optimization methods.

REFERENCES

[1] K. Choi, D.-H. Jang, S.-I. Kang, J.-H. Lee, T.-K. Chung, and H.-S. Kim, "Hybrid algorithm combing genetic algorithm with evolution strategy for antenna design," *IEEE Trans. Magn.*, vol. 52, no. 3, Mar. 2016, Art. no. 7209004.

[2] Z. Lin, M. Yao, and X. Shen, "Sidelobe reduction of the low profile multi-subarray antenna by genetic algorithm," *AEU-Int. J. Electron. Commun.*, vol. 66, no. 2, pp. 133–139, 2012.

[3] Y.-L. Li, W. Shao, L. You, and B.-Z. Wang, "An improved PSO algorithm and its application to UWB antenna design," *IEEE Antennas Wireless Propag. Lett.*, vol. 12, pp. 1236–1239, Oct. 2013.

[4] J. Dong, Q. Li, and L. Deng, "Design of fragment-type antenna structure using an improved BPSO," *IEEE Trans. Antennas Propag.*, vol. 66, no. 2, pp. 564–571, Feb. 2018.

[5] Y.-L. Li, W. Shao, J.-T. Wang, and H. Chen, "An improved NSGA-II and its application for reconfigurable pixel antenna design," *Radioengineering*, vol. 23, no. 2, pp. 733–738, 2014.

[6] M. John and M. J. Ammann, "Antenna optimization with a computationally efficient multiobjective evolutionary algorithm," *IEEE Trans. Antennas Propag.*, vol. 57, no. 1, pp. 260–263, Jan. 2009.

[7] S. Koziel and S. Ogurtsov, "Multi-objective design of antennas using variable-fidelity simulations and surrogate models," *IEEE Trans. Antennas Propag.*, vol. 61, no. 12, pp. 5931–5939, Dec. 2013.

[8] S. Koziel, A. Bekasiewicz, and W. Zieniutycz, "Expedited EM-driven multiobjective antenna design in highly dimensional parameter spaces," *IEEE Antennas Wireless Propag. Lett.*, vol. 13, pp. 631–634, 2014.

[9] S. Koziel and A. Bekasiewicz, "Fast multi-objective surrogate-assisted design of multi-parameter antenna structures through rotational design space reduction," *IET Microw., Antennas Propag.*, vol. 10, no. 6, pp. 624–630, 2016.

[10] J. Dong, Q. Li, and L. Deng, "Fast multi-objective optimization of multi-parameter antenna structures based on improved MOEA/D with surrogate-assisted model," *AEU-Int. J. Electron. Commun.*, vol. 72, pp. 192–199, Feb. 2017.

[11] S. Koziel, A. Bekasiewicz, and S. Szczepanski, "Multi-objective design optimization of antennas for reflection, size, and gain variability using kriging surrogates and generalized domain segmentation," *Int. J. RF Microw. Comput.-Aided Eng.*, vol. 28, no. 5, 2018, Art. no. e21253.

[12] B. Liu, H. Aliakbarian, Z. Ma, G. A. E. Vandenbosch, G. Gielen, and P. Excell, "An efficient method for antenna design optimization based on evolutionary computation and machine learning techniques," *IEEE Trans. Antennas Propag.*, vol. 62, no. 1, pp. 7–18, Jan. 2014.

[13] J. P. Jacobs, "Efficient resonant frequency modeling for dual-band microstrip antennas by Gaussian process regression," *IEEE Antennas Wireless Propag. Lett.*, vol. 14, pp. 337–341, 2015.

[14] L.-L. Chen, C. Liao, W. Lin, L. Chang, and X.-M. Zhong, "Hybrid-surrogate-model-based efficient global optimization for high-dimensional antenna design," *Prog. Electromagn. Res.*, vol. 124, no. 8, pp. 85–100, 2012.

[15] T. Khan, A. De, and M. Uddin, "Prediction of slot-size and inserted air-gap for improving the performance of rectangular microstrip antennas using artificial neural networks," *IEEE Antennas Wireless Propag. Lett.*, vol. 12, pp. 1367–1371, 2013.

[16] A. P. Anuradha and S. N. Sinha, "Design of custom-made fractal multi-band antennas using ANN-PSO," *IEEE Antennas Propag. Mag.*, vol. 53, no. 4, pp. 94–101, Aug. 2011.

[17] H. Aliakbari, A. Abdipour, A. Costanzo, D. Masotti, R. Mirzavand, and P. Mousavi, "ANN-based design of a versatile millimetre-wave slotted patch multi-antenna configuration for 5G scenarios," *IET Microw., Antennas Propag.*, vol. 11, no. 9, pp. 1288–1295, 2017.

[18] D. R. Jones, "A taxonomy of global optimization methods based on response surfaces," *J. Global Optim.*, vol. 21, no. 4, pp. 345–383, 2001.

[19] A. Massa, G. Oliveri, M. Salucci, N. Anselmi, and P. Rocca, "Learning-by-examples techniques as applied to electromagnetics," *J. Electromagn. Waves Appl.*, vol. 32, no. 4, pp. 516–541, 2018.

[20] N. P. Somasiri, X. Chen, and A. A. Rezazadeh, "Neural network modeller for design optimisation of multilayer patch antennas," *IEE Proc.-Microw. Antennas Propag.*, vol. 151, no. 6, pp. 514–518, 2004.

[21] N. Jin and Y. Rahmat-Samii, "Hybrid real-binary particle swarm optimization (HPSO) in engineering electromagnetics," *IEEE Trans. Antennas Propag.*, vol. 58, no. 12, pp. 3786–3794, Dec. 2010.

[22] K. Deb, *Multi-Objective Optimization Using Evolutionary Algorithms*. New York, NY, USA: Wiley, 2001.

[23] D. E. Rumelhart, G. E. Hinton, and R. J. Williams, "Learning representations by back-propagating errors," *Nature*, vol. 323, pp. 533–536, Oct. 1986.

[24] K. Hornik, M. Stinchcombe, and H. White, "Multilayer feedforward networks are universal approximators," *Neural Netw.*, vol. 2, no. 5, pp. 359–366, 1989.

[25] J.-R. Zhang, J. Zhang, T.-M. Lok, and M. R. Lyu, "A hybrid particle swarm optimization–back-propagation algorithm for feedforward neural network training," *Appl. Math. Comput.*, vol. 185, no. 2, pp. 1026–1037, 2007.

[26] S. Saremi, S. Mirjalili, and A. Lewis, "How important is a transfer function in discrete heuristic algorithms," *Neural Comput. Appl.*, vol. 26, no. 3, pp. 625–640, 2015.

[27] M. Stein, "Large sample properties of simulations using Latin hypercube sampling," *Technometrics*, vol. 29, no. 2, pp. 143–151, 1987.
[28] A. B. Owen, "A central limit theorem for Latin hypercube sampling," *J. Roy. Stat. Soc.*, vol. 54, no. 2, pp. 541–551, 1992.
[29] J. Dong, W. Qin, Y. Li, Q. Li, and L. Deng, "Fast multi-objective antenna design based on improved back propagation neural network surrogate model," (in Chinese), *J. Electron. Inf. Technol.*, vol. 40, no. 11, pp. 2712–2719, 2018.
[30] Q. Zhang and H. Li, "MOEA/D: A multiobjective evolutionary algorithm based on decomposition," *IEEE Trans. Evol. Comput.*, vol. 11, no. 6, pp. 712–731, Dec. 2007.

JIAN DONG received the B.S. degree in electrical engineering from Hunan University, Changsha, China, in 2004, and the Ph.D. degree in electrical engineering from the Huazhong University of Science and Technology (HUST), Wuhan, China, in 2010. From 2006 to 2010, he was a Research Assistant with the National Key Laboratory of Science and Technology on Multispectral Information Processing, HUST. From 2016 to 2017, he was a Visiting Scholar with the ELEDIA Research Center of the University of Trento, Italy. Since 2010, he has been an Associate Professor with the School of Information Science and Engineering, Central South University, Changsha, China. He holds 15 innovation patents and has published 6 books and over 100 peer reviewed papers on international journals and conferences. His current research interests include antennas, wireless communications, and numerical optimization techniques.

WENWEN QIN received the B.S. degree from Central South University, Changsha, China, in 2015. She is currently pursuing the M.S. degree with Central South University. Her research interests include antenna optimization techniques and multiband/wideband antenna designs.

MENG WANG received the B.S. and M.S. degrees in electrical engineering from Northwestern Polytechnic University, Beijing University of Posts and Telecommunications, in 2010 and 2013, respectively, and the Ph.D. degree from North Carolina State University at Raleigh, in 2017. She is currently a Lecturer with the School of Computer Science at Central South University, China. Her research interests include reconfigurable antennas, liquid metal antennas, and their potential applications in portable electronic devices.